



Experimental and Numerical Studies on the Effect of Rainfall on Triggering Shallow Landslides

Binod Tiwari, Katsuyuki Kawai, Adam Lewis, and Phommachanh Viradeth

Abstract

Rainfall is considered one of the major triggering factors for shallow landslides. The effect of rainfall in causing landslides depends on the intensity and duration of rainfall, the type of soil, the inclination of the slope, and ground water conditions. The majority of slope stability problems in shallow slides involve partially saturated soils. Although experimental modelling of slopes subjected to various intensities and durations of rainfall are ideal to evaluate the effect of rainfall on slope stability, it is time consuming and expensive. Numerical simulation of such experimental modelling can save a great deal of time and cost. In this study, slope models were prepared at angles of inclination of 30° and 45° with double washed construction sand, at a void ratio of 0.7. The slopes were subjected to 30 mm/h of rainfall for 3 h. Spatial variation of suction during the rainfall and depth of water front with time were measured for the entire rainfall period. The depth of water front and spatial variation of suction were also calculated through the finite element model (FEM) that was developed based on a hydro-mechanical model developed for the partially saturated soil. The numerical and experimental results provided identical results. The numerical result was extended to predict the spatial variation of suction, depth of water front and deformation of slope subjected to higher intensity of rainfall.

Keywords

Partially saturated soil • Suction • Water front • Finite element analysis • Rainfall intensity • Slope stability

Background

Damage caused by rainfall-triggered shallow landslides is well documented in the literature. Although shallow landslides are caused by various factors such as rainfall, earthquakes, and anthropogenic causes, statistics show that rainfall-induced shallow landslides are much frequent than landslides triggered by other factors. Fukuoka (1980) reported that the annual number of documented landslides in Japan exceed 10,000, and could reach 100,000, if documented properly. Similar numbers of shallow landslides are reported all over the world. The depth and steepness of shallow landslides are reported to be 0.5–2 m and 30–50°, respectively. Significant monitoring and warning systems

B. Tiwari (✉)
Department of Civil and Environmental Engineering, California State University Fullerton, 800 N State College Blvd., Fullerton, CA 92831, USA
e-mail: btiwari@fullerton.edu

K. Kawai • P. Viradeth
Department of Civil Engineering, Kobe University, 1-1 Rokkoudaicho Nadaku, Kobe 657-0013, Japan
e-mail: kkawai@kobe-u.ac.jp; pviradeth@gmail.com

A. Lewis
GeoStabilization International, P.O. Box 4709, Grand Junction, CO 81502, USA
e-mail: adam@gsi.us

have been implemented in various countries including USA, Japan, and Italy, in order to predict potential shallow sliding based on the calculated threshold rainfall amounts.

Various studies that have been conducted to evaluate the effect of rainfall on the stability of shallow slides loosely incorporate seepage conditions for partially saturated soils. Moreover, the numerical simulation results have not been verified with the experimental or field data. In this study, we conducted experimental studies on the change in the depth of water front and suction in soil with time and verified the results with the results obtained from the fully coupled hydro-mechanical model that was developed for partially saturated soils. The numerical results were further utilized to predict the velocity of movement of the water front based on the intensity and duration of rainfall at different inclinations of slopes. In this paper, the experimental modelling results are described briefly, but the numerical modelling results are described in more detail.

Materials and Methods

Experimental Modeling

Experimental models were prepared with double washed sand. The proportion of sand was approximately 95 %, with approximately 5 % fines. The soil was classified as SW material according to USCS. Specific gravity of the sand was 2.65. The horizontal and vertical coefficients of permeability of the sand were 8.0×10^{-3} and 4.3×10^{-3} cm/s, respectively. Soil water retention characteristic curves were prepared by measuring suctions in soil samples that were prepared in a 30 cm \times 30 cm \times 30 cm containers at different degrees of saturation, both for dry to wet and wet to dry cycles. A 1.22 m \times 1.22 m \times 1.22 m sized Plexiglas container was used to prepare the models. The Plexiglas container provides visibility to observe the depth of the water front at various durations of rainfall. The rain simulator used in this study was made of 16 special sprinkler heads arranged in such a way that the flow of water could be controlled in the sprinkler system in order to vary the intensity of rainfall from 18 to 360 mm/h. Separate slope models were prepared at angles of inclination of 30° and 45° by compacting soil in the container at the void ratio of 0.7 (corresponding relative density of 30 %). The experimental set-up is shown in Fig. 1. Four tensiometers were installed in the slopes, as shown in Fig. 2, in order to measure the spatial variation in suction with the duration of rainfall. The tensiometers used in this study were miniature tensiometers with a 0.5 cm² surface area and 5 mm tip size (T5 type), supplied by Decagon Devices. The tensiometer can measure pore pressures ranging from -100 kPa to $+85$ kPa with an accuracy of -0.5 kPa. Each slope was subjected to a rainfall



Fig. 1 Plexiglas container, slope made of double washed sand at a 30° inclination, and the rain simulator used in this study

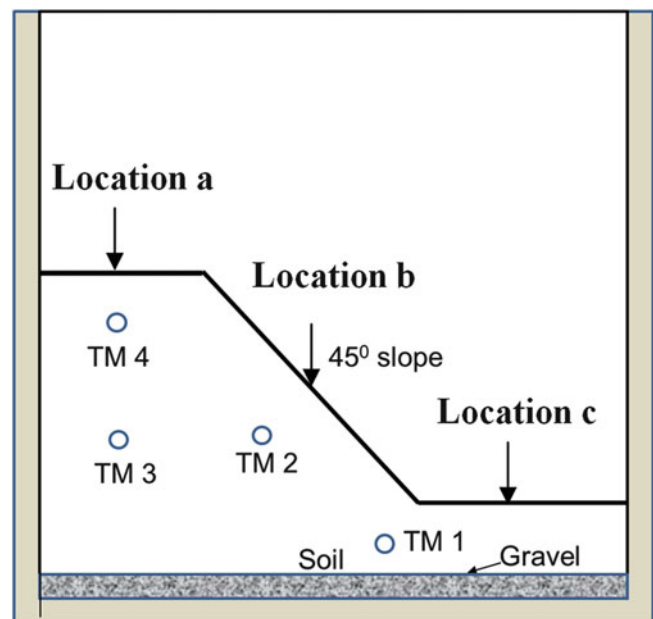


Fig. 2 Location of tensiometers within the slope

having an intensity of 30 mm/h for 3 h. The movement of the water front was marked at the boundary of the slope around the Plexiglas container every 15 min and the values of suction were recorded every minute.

Numerical Modeling

The soil-water-air coupled hydro-mechanical model developed by Kawai et al. (2007) was used in this study. Soil water retention characteristics curves were used to calculate the relationship between moisture content and suction.

The procedure proposed by Kawai et al. (2009), based on the approach recommended by Sugii and Uno (1996), was utilized to evaluate the parameters of the soil water retention characteristics of the tested soil sample. The equation utilized for the shape of drying and wetting cycles, i.e., the hysteresis of the soil water retention characteristics curves are presented in Eq. (1).

$$\frac{S_r - S_{rc}}{S_{rf} - S_{rc}} = \frac{1}{1 + \exp(A + B \log_e s)} \quad (1)$$

where,

S_r is degree of saturation; S_{rf} is degree of saturation at $s \rightarrow 0$; S_{rc} is degree of saturation at $s \rightarrow \infty$; s is initial suction; and A and B are curve-fitting parameters.

In this study, a soil/water/air coupled finite element analysis program was developed to evaluate the effect of rainfall on the variation in suction. Darcy's law applies for coefficients of permeability of both water and air. The relationships developed, as presented in Eqs. 2 and 3, were utilized in this study.

Darcy's law for water permeability is calculated as:

$$\mathbf{v}_w = -\mathbf{K}_w \cdot \text{grad } h = -k_{rw} \mathbf{k}_w \cdot \text{grad } h \quad (2)$$

$$\text{Here, } \text{grad } h = \frac{\partial h}{\partial x} + \frac{\partial h}{\partial y}$$

Darcy's law for air permeability is calculated as:

$$\mathbf{v}_a = -\mathbf{K}_a \cdot \text{grad} \left(\frac{P_a}{\rho_w g} \right) = -k_{ra} \mathbf{k}_a \cdot \text{grad} \left(\frac{P_a}{\rho_w g} \right) \quad (3)$$

$$\text{Here, } \text{grad} \left(\frac{P_a}{\rho_w g} \right) = \frac{\partial \left(\frac{P_a}{\rho_w g} \right)}{\partial x} + \frac{\partial \left(\frac{P_a}{\rho_w g} \right)}{\partial y}$$

Several functions of water and air permeability have been proposed in the literature. In this study, the equation proposed by Mualem (1974) for water permeability and the equation proposed by Van Genuchten (1980) for air permeability of unsaturated soil were used. The equations for the ratios of water and air permeability with the permeability of saturated soil (K_{rw} and K_{ra} respectively, herein after referred as the relative coefficient of permeability) are presented in Eqs. 4 and 5, respectively. Water permeability of soil is:

$$k_{rw} = S_e^{\frac{1}{2}} \left[1 - \left(1 - S_e^{\frac{1}{m}} \right)^m \right]^2 \quad (4)$$

Air permeability is calculated as:

$$k_{ra} = (1 - S_e)^\gamma \left(1 - S_e^{\frac{1}{m}} \right)^{2m} \quad (5)$$

where, m is Mualem's coefficient, which is taken as 0.8 in this study; γ is a shape parameter, which ranges between 0.33 and 0.50, and S_e is effective degree of saturation.

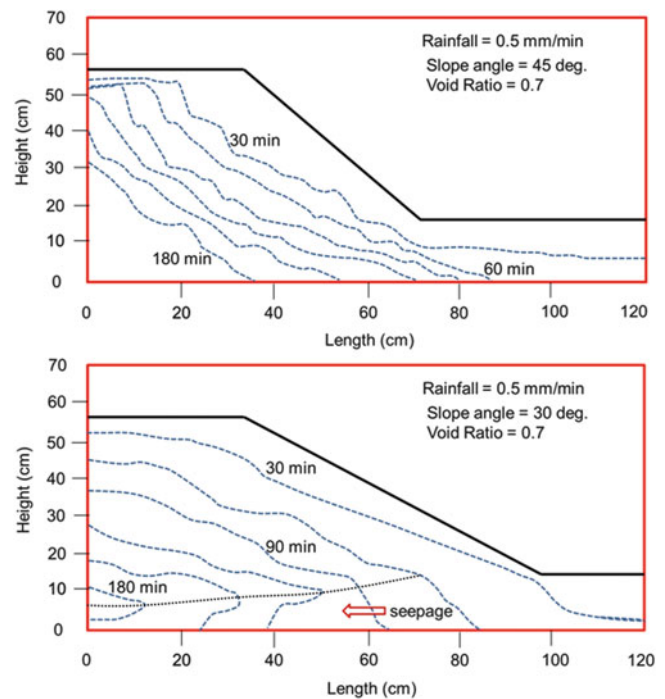


Fig. 3 Depth of water front at different durations of rainfall in model numbers 8 (top) and 7 (bottom)

Results of the Study

Experimental Modeling

The variation in the depth of water front that was recorded at 30 min intervals in slopes having angles of inclinations of 45° and 30° are presented in Fig. 3. As it can be seen in Fig. 3, the rate of movement of the water front within the slope is much faster than the rate of movement of water front in the flat portion at the top of the slope. This can be attributed to the movement of water in an inclined direction, especially for the saturated soil above the water front. However, the angle of inclination of the water front was less than the angle of inclination of the slopes. In the case of the slope with a 30° angle of inclination, it was observed that once the flat portion near the toe became saturated, it completely filled the drainage layer and started to supply water in the horizontal direction as well. Therefore, the data below the dotted line (indicated as seepage) is not considered for further analysis.

Figure 4 illustrates the values of suction observed at four locations, as described in Fig. 2. The initial suction at the four locations prior to rainfall ranged from 5.5 to 6.5 kPa. The soil at the top (near tensiometer #4) required approximately 60 min to reduce the suction close to 0 kPa, whereas the soil near the bottom of the slope (near tensiometer #1) required almost 120 min to drop the suction to 0 kPa. Please

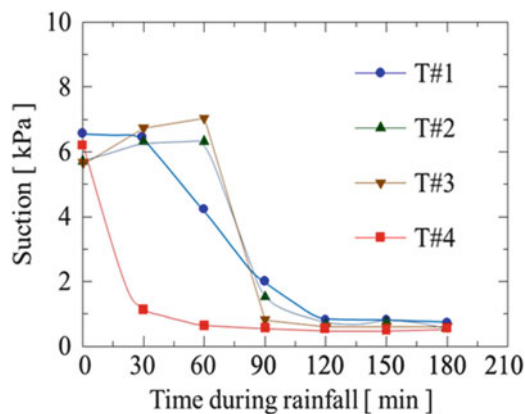


Fig. 4 Variation in suction with the duration of rainfall at locations described in Fig. 2 for a 45° slope

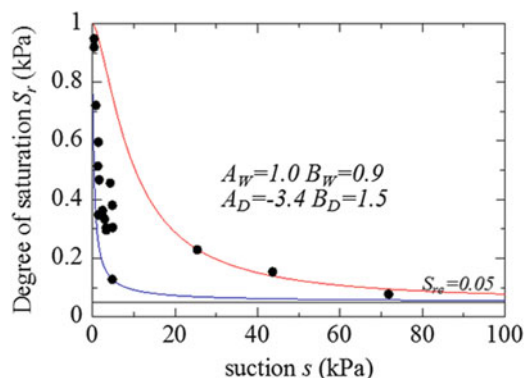


Fig. 5 Soil water retention characteristics curves of tested sample, derived from lab test

note that due to the sensitivity of the tensiometer used in this study (i.e. ± 0.5 kPa), measured suction may give an error of up to 0.5 kPa. The tensiometers installed at the other two locations within the slope also needed more than 60 min to become saturated. The rates of change in suction with time at all four locations were different. Locations near tensiometers 2 and 3 showed a similar pattern in the reduction of suction with time. The results presented in Fig. 4 show that the water fronts were not able to progress to tensiometer # 1 in 30 min and to tensiometers #s 2 and 3 in 60 min after the initiation of rainfall.

Numerical Modeling

Shown in Fig. 5 is the soil water retention characteristics curves prepared for both wetting and drying cycles of the degree of saturation–suction relationship curve. Equation 1 represents the regression curves for both dry and wet cycles. The suction parameters A and B (Eq. 1) were calculated for both drying and wetting cycles using the experimentally

derived values, as presented in Fig. 5. These parameters were used to calculate the values of suction in soil at different degrees of saturation during the numerical simulation.

Equations 1 through 5 were combined to calculate the depth of the water front during rainfall, and corresponding values of the degree of saturation and suction. Presented in Fig. 6 are the spatial distributions of suction in slopes with angles of inclination of 45° and 30°, compacted at a void ratio of 0.7, prior to rainfall. Suction ranged from 5.5 to 6.5 kPa in both slopes. Presented in Fig. 7 are the values of suction in those slopes after the application of 30 mm/h of rainfall for 3 h. The depth of water front, depicted by zero suction, can be seen in both figures. As expected, the depth of water front was higher in the steeper slope. Once the water saturates the toe of the slope, water starts to flow towards the slope in a horizontal direction as a result of a significantly high coefficient of permeability of gravel (drainage layer). Based on the numerical simulation result, the movement of the water front appeared to be parallel to the slope until the soil at the right side of the toe was fully saturated with rain water. After that, the soil close to the toe received water from rainfall as well as the seepage water from the saturated soil mass below the toe. This caused a slight deviation in the shape of the water front from the shape before the toe became saturated. The effect, right after 3 h of rainfall, is more pronounced in the slope with an inclination of 45° compared to the slope having an inclination of 30°.

Comparison between the numerically computed and experimentally observed values of the depths of the water front for a 45° slope after 30, 60, 90, and 180 min of rainfall are presented in Fig. 8a–d, respectively. Figure 8 also includes the numerically simulated values of the depths of the water front for the intensities of rainfall of 1.0 mm/min and 1.5 mm/min, whichever are applicable. The calculated and observed locations of the depth of the water front were very close near the flat portions on top of the slope (location a, Fig. 2) and bottom of the slope (location c, Fig. 2). However, the actual location of water front was lower than the front predicted by the numerical simulation within the inclined portion of the slope (location b, Fig. 2). Similarly, the location of the water front was slightly higher than the numerically simulated position in the case of location a, but was lower than the numerically simulated positions at location b for the durations of 60, 90, and 180 min of rainfall. The experimentally observed and numerically simulated positions of water front were close at location c for 60, 90 and 180 min of rainfall. Similar results were obtained for the 30° slope.

Comparison between the suctions obtained with the numerical simulation and model experiments for four different locations T1, T2, T3, and T4, described in Fig. 2, are presented in Fig. 9a–d, respectively. The numerical values differed from the observed values by less than 0.5 kPa. In the

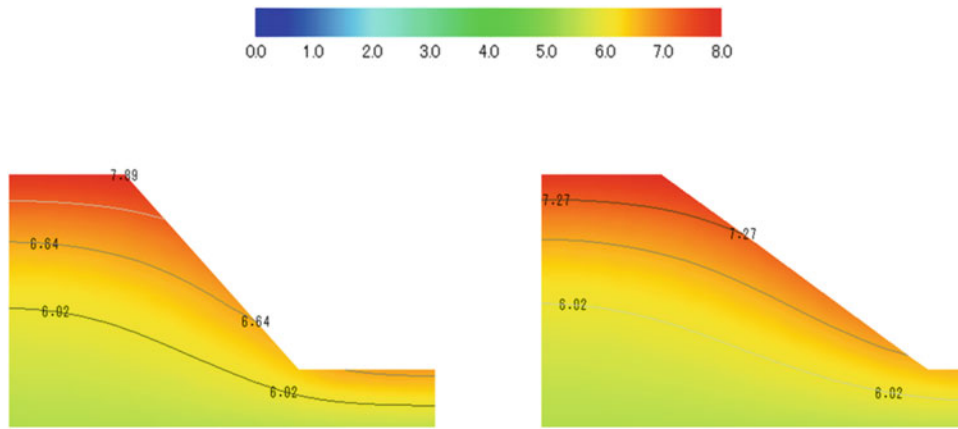


Fig. 6 Variation of suction in slopes prior to rainfall—(left) 45° slope, (right) 30° slope

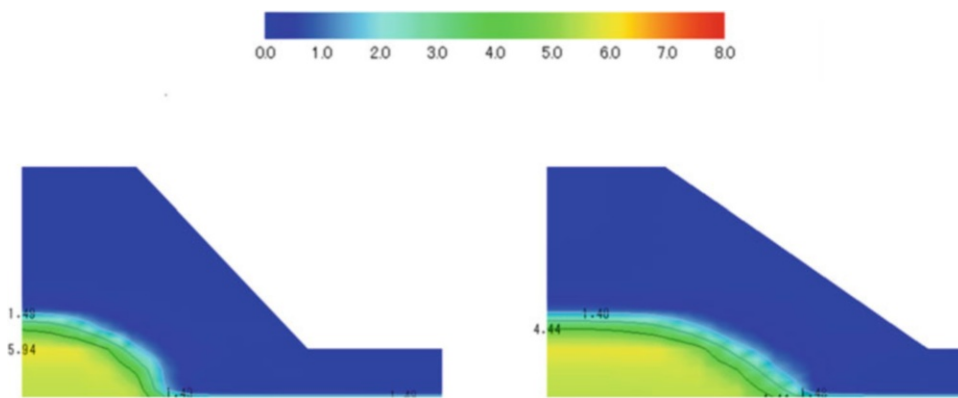


Fig. 7 Variation of suction in slopes after 3 h of rainfall—(left) 45° slope, (right) 30° slope

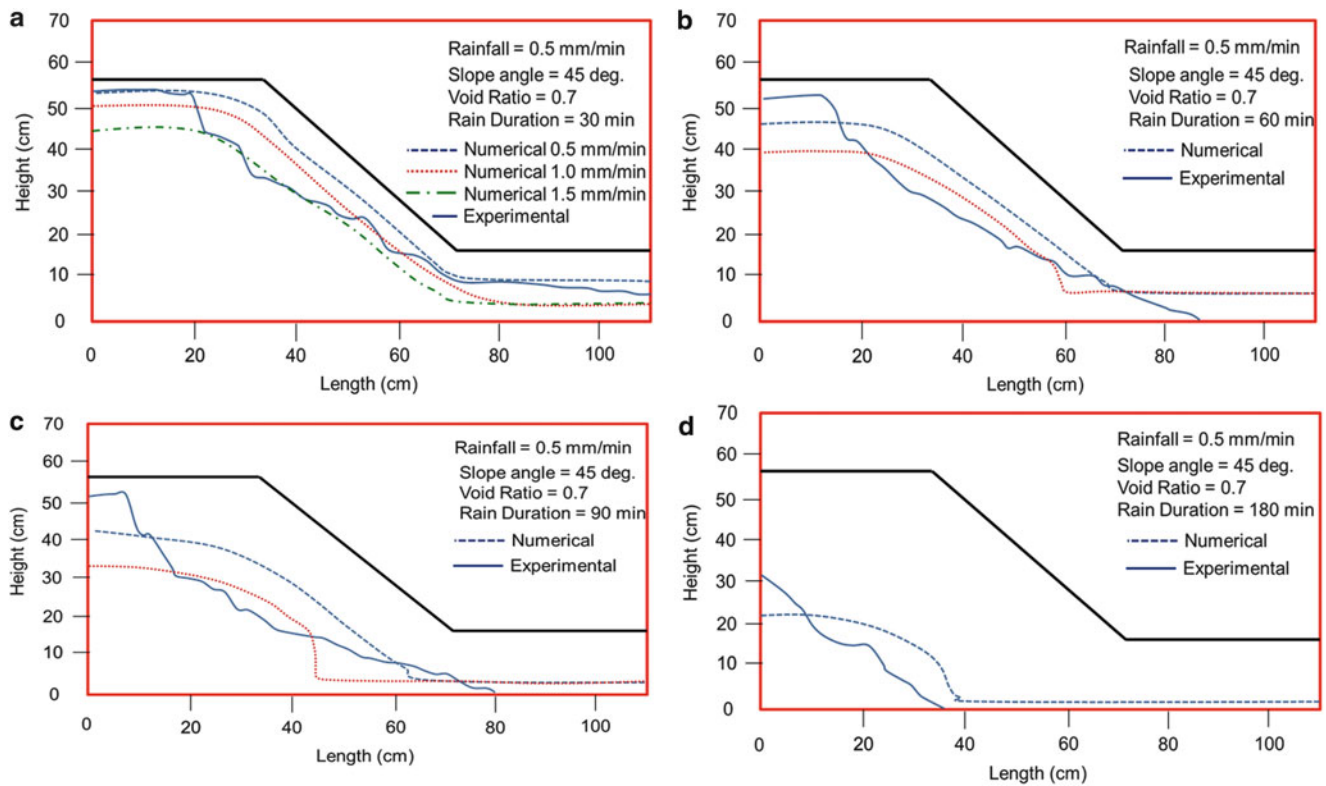
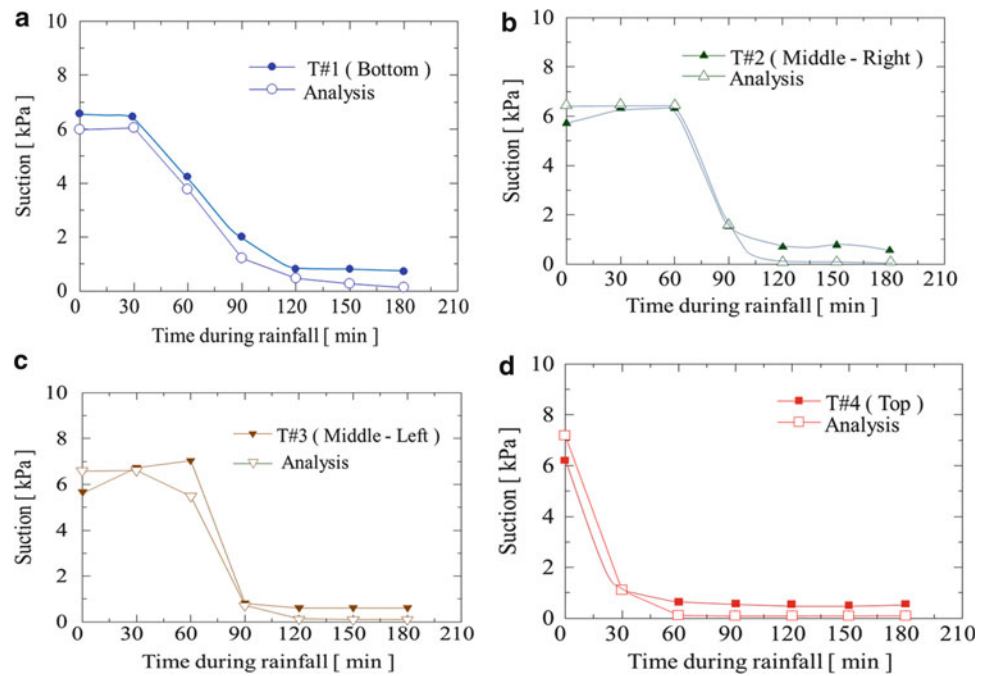


Fig. 8 Experimentally observed and numerically simulated positions of water front for different durations of rainfall

Fig. 9 Comparison between the experimental and numerical values of the suction at different locations (see Fig. 2)



majority of the cases, the numerical calculations showed lower suction values. Considering the precision of the tensiometer (i.e. ± 0.5 kPa), the numerically calculated values are considered to be reasonably accurate. This shows that the proposed numerical modeling technique can be utilized with reasonable accuracy to calculate the spatial distribution of suction in slopes during rainfall on partially saturated slopes.

Summary and Conclusions

Experimental and numerical modelling were conducted in order to investigate the variation in the depth of the water front and spatial distribution of suction in sandy slopes with two different inclinations during a rain event that produced 30 mm/h of rainfall for 3 h. The model developed by the authors that incorporated a hydro-mechanical coupled analysis for partially saturated soil with a finite element modelling technique was able to predict the depth of the water front and variation in suction with reasonable accuracy. This model was also utilized to evaluate the depth of the water front and variation in suction as well as a deformation analysis of slope for various intensities and durations of rainfall.

Acknowledgments The authors would like to thank the Associated Student Inc. (ASD), California State University, Fullerton, for providing financial support to purchase materials.

References

- Fukuoka M (1980) Landslides associated with rainfall. *Geotech Eng J Southeast Asia Soc Soil Eng* 11:1–29
- Kawai K, Iizuka A, Hayakawa E, Wang W (2007) Non-uniform settlement of compacted earth structures caused by the deformation characteristics of unsaturated soil on wetting. *Soils Found* 47 (2):195–205
- Kawai K, Iizuka A, Tachibana S, Ohno S (2009) Impacts of plant induced uptake on the stability of earth structure. In: *Proceedings of international conference on soil mechanics and geotechnical engineering*, Alexandria, Egypt, pp 526–529
- Mualem Y (1974) A conceptual model of hysteresis. *Water Resour Res* 10(3):514–520
- Sugii T, Uno T (1996) Modeling of hydraulic properties for unsaturated soils. In: *Proceedings of symposium on permeability of unsaturated ground*, pp 179–184 (in Japanese)
- Van Genuchten M (1980) A closed form equation for predicting hydraulic conductivity of unsaturated soils. *J Soil Sci Soc Am* 44:892–898